Net carbon dioxide losses of northern ecosystems in response to autumn warming

Shilong Piao, Philippe Ciais, Pierre Friedlingstein, Philippe Peylin, Markus Reichstein, Sebastiaan Luyssaert, Hank Margolis, Jingyun Fang, Alan Barr, Anping Chen, et al.

Net carbon dioxide losses of northern ecosystems in response to autumn warming

Shilong Piao[1], Philippe Ciais[1], Pierre Friedlingstein[1], Philippe Peylin[2], Markus Reichstein[3], Sebastiaan Luyssaert[4], Hank Margolis[5], Jingyun Fang[6], Alan Barr[7], Anping Chen[8], Achim Grelle[9], David Y. Hollinger[10], Tuomas Laurila[11], Anders Lindroth[12], Andrew D. Richardson[13] & Timo Vesala[14]

[1]LSCE, UMR CEA-CNRS, Bâtiment 709, CE, L'Orme des Merisiers, F-91191 Gif-sur-Yvette, France
[2]Laboratoire de Biogéochimie Isotopique, LBI, Bâtiment EGER, F-78026 ThivervalGrignon, France
[3]Max Planck Institute for Biogeochemistry, PO Box 100164, 07701 Jena, Germany
[4]Department of Biology, University of Antwerp, Universiteitsplein 1, 2610 Wilrijk, Belgium
[5]Faculté de foresterie et de géomatique, Université Laval, Sainte-Foy, Quebec G1K 7P4, Canada
[6]Department of Ecology, Peking University, Beijing 100871, China
[7]Climate Research Division, Environment Canada, 11 Innovation Boulevard, Saskatoon, Saskatchewan S7N 3H5, Canada
[8]Department of Ecology and Evolutionary Biology, Princeton University, Princeton, New Jersey 08544, USA
[9]Department of Ecology, Swedish University of Agricultural Sciences, SE-750 07 Uppsala, Sweden
[10]USDA Forest Service Northern Research Station, 271 Mast Road, Durham, New Hampshire 03824, USA
[11]Finnish Meteorological Institute, FIN-00101 Helsinki, Finland
[12]Department of Physical Geography and Ecosystems Analysis, Lund University, SE-22362 Lund, Sweden
[13]Complex Systems Research Center, University of New Hampshire, Durham, New Hampshire 03824, USA
[14]Department of Physical Sciences, University of Helsinki, PO Box 64, FIN-00014 Helsinki, Finland

The carbon balance of terrestrial ecosystems is particularly sensitive to climatic changes in autumn and spring[1–4], with spring and autumn temperatures over northern latitudes having risen by about 1.1 °C and 0.8 °C, respectively, over the past two decades[5]. A simultaneous greening trend has also been observed, characterized by a longer growing season and greater photosynthetic activity[6,7]. These observations have led to speculation that spring and autumn warming could enhance carbon sequestration and extend the period of net carbon uptake in the future[8]. Here we analyse interannual variations in atmospheric carbon dioxide concentration data and ecosystem carbon dioxide fluxes. We find that atmospheric records from the past 20 years show a trend towards an earlier autumn-to-winter carbon dioxide build-up, suggesting a shorter net carbon uptake period. This trend cannot be explained by changes in atmospheric transport alone and, together with the ecosystem flux data, suggest increasing carbon losses in autumn. We use a process-based terrestrial biosphere model and satellite vegetation greenness index observations to investigate further the observed seasonal response of northern ecosystems to autumnal warming. We find that both photosynthesis and respiration increase during autumn warming, but the increase in respiration is greater. In contrast, warming increases photosynthesis more than respiration in spring. Our simulations and observations indicate that northern terrestrial ecosystems may currently lose carbon dioxide in response to autumn warming, with a sensitivity of about 0.2 PgC °C^{-1}, offsetting 90% of the increased carbon dioxide uptake during spring. If future autumn warming occurs at a faster rate than in spring, the ability of northern ecosystems to sequester carbon may be diminished earlier than previously suggested[9,10].

The carbon balance of terrestrial ecosystems is highly sensitive to climate changes at the edges of the growing season[1–4]. In response to warmer springs, for example, several field studies have shown that boreal forests absorb more carbon[11,12] as a result of an earlier beginning of the growing season[13,14]. A strong autumn warming is currently occurring in eastern Asia and eastern North America[15]. However, little

attention has been given to the impacts of this forcing on the terrestrial carbon cycle. We have analysed how interannual variations and trends in autumn temperatures have recently affected atmospheric CO_2 concentrations, ecosystem CO_2 fluxes measured by eddy covariance, and remotely sensed vegetation greenness values. A process-oriented terrestrial biosphere model (ORCHIDEE)[16] is combined with an atmospheric transport model (LMDZt)[17] to quantify the processes through which autumn warming controls the carbon balance of ecosystems (see Methods).

The seasonal cycle of atmospheric CO_2 concentrations provides an integrated measure of the net land–atmosphere carbon exchange (net ecosystem productivity; NEP) and its temporal characteristics[18,19]. We analysed the ten atmospheric CO_2 measurement records from the NOAA–ESRL air-sampling network[20], which cover at least 15 years of data in the Northern Hemisphere (Fig. 1 and Supplementary Table 1).

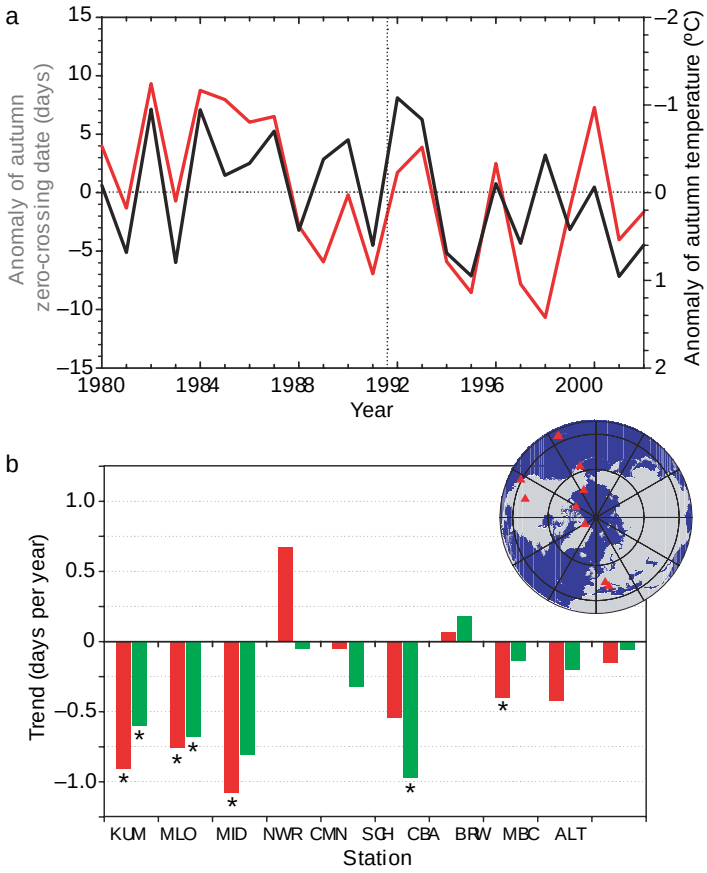

Figure 1 — Atmospheric CO_2 concentration data analysis from long-term records of the global NOAA-ERSL air-sampling network. a, Interannual variability in anomaly of upward zero-crossing date (red) observed at Point Barrow, Alaska, and the corresponding autumn (September to November) temperature (black) over the region between 51° and 90° N over the past two decades. Upward zero-crossing date is strongly anti-correlated with autumn temperature (slope = – 5.4 days $°C^{-1}$; R = 0.61, P = 0.002). The vertical dotted line indicates the time of the eruption of Mount Pinatubo. b, Trends in upward zero-crossing date (red) and length of the net CUP (green) from long-term Northern Hemisphere atmospheric observations during at least the past 15 years (see Methods). The differences in the trends between autumn upward zero-crossing date and CUP reflects changes in the spring downward zero crossing. As a result of the earlier autumn upward zero-crossing date, CUP has persistently decreased by an average of 0.36 ± 0.38 days per year since 1980. The inset shows the distribution of the stations used in this study. Station abbreviations are defined in Supplementary Table 1.

The upward zero-crossing date of CO_2 was determined as the day when the de-trended atmospheric CO_2 seasonal cycle crosses the zero line from negative to positive values (see Methods). This date occurs in

autumn at northern high-latitude stations and in early winter at northern tropical stations (Supplementary Table 1). We found that variations in the CO_2 zero-crossing date are negatively correlated with anomalies in autumn air temperatures[5] over a broad region surrounding each station by 620u of latitude. All CO_2 records show a negative correlation, with four out of ten sites having statistically significant correlations (Supplementary Table 2). The probability that this occurs purely by chance is estimated to be about 1025 if all station records are assumed to be independent (see Supplementary Information). The striking anticorrelation between autumnal temperature and CO_2 zero-crossing date is illustrated in Fig. 1a for the 23-year-long atmospheric measurement record of Point Barrow in northern Alaska ($R = -0.61$, $P = 0.002$). In contrast with the widespread influence of temperature, the upward CO_2 zero-crossing date shows no significant correlation with precipitation anomalies (Supplementary Table 2). If soil moisture calculated by the ORCHIDEE model (see Methods) is used instead of precipitation as a predictor of CO_2 upward zero-crossing dates, then only six of the ten sites show a positive correlation, and only three of the ten sites show a higher correlation with soil moisture than with temperature. Similar results are also inferred from a partial correlation analysis in which the controlling effects of other variables on temperature were removed (Supplementary Table 2).

We verified that the strong negative correlation between upward CO_2 zero-crossing date and temperature predominantly reflects climate-driven fluctuations in NEP, rather than interannual fluctuations in atmospheric transport. To do so, we prescribed either variable NEP or climatological NEP fluxes from ORCHIDEE to the global transport model LMDZt driven by variable wind fields (see Methods). With the exception of the Mt Cimone (CMN) and Cape Kumukahi (KUM) stations, we found that the fluctuations in upward zero-crossing dates are driven mainly by changes in NEP, and only partly by interannual wind changes (see Methods, Supplementary Table 3 and Supplementary Fig. 1). We also verified that accounting for increasing ocean uptake and fossil fuel emissions in the LMDZt transport model did not significantly affect the zero-crossing dates because these two fluxes contribute less than 4% of the variation for all sites (except for station KUM). The possible changes in seasonal fossil fuel emissions over time may only marginally impact the upward CO_2 zero-crossing date changes (see Methods).

There is also a long-term trend in the autumn upward zero-crossing date of atmospheric CO_2 superimposed on interannual fluctuations. At Point Barrow, for instance, we determined a systematic advance of -0.40 day yr^{-1} (Fig. 1b), which was not primarily caused by changes in atmospheric transport, because the trends in zero-crossing date simulated with climatological ORCHIDEE fluxes and interannual transport are only about -0.12 day yr^{-1}. Overall, eight of ten sites show an earlier trend in upward zero-crossing date, with four sites being statistically significant (Fig. 1b). This trend towards earlier or increased ecosystem losses of CO_2 in autumn becomes apparent when analysing CO_2 data from the past decade, whereas it was non-existent in the CO_2 data from 1970 to 1994 (ref. 18) as a result of the time-frame of their analysis. This trend towards larger autumn CO_2 losses is not a legacy from drier summers[21], because atmospheric CO_2 data show that weaker summer CO_2 minima are not significantly associated with an advanced upward zero-crossing date at all sites. The advance in autumnal atmospheric CO_2 zero-crossing date clearly exceeds that of the spring zero-crossing date (Supplementary Table 3). Thus, the duration of the net carbon uptake period (CUP), defined as the difference between autumn upward and spring downward CO_2 zero-crossing dates, has on average decreased at nearly all Northern Hemisphere atmospheric CO_2 stations (Fig. 1b).

Next, we analysed 108 site-years of eddy-covariance CO_2 measurement data from 24 northern ecosystem sites (Supplementary Table 4) to quantify the response of the CUP ending date to interannual variations in autumn temperature (see Methods). All sites combined show that the CUP terminates

systematically earlier when autumn conditions are warmer, and vice versa (Fig. 2). Further, stronger temperature anomalies seem to have stronger effects on ecosystem carbon balance than weak anomalies ($P < 0.05$). Hence, despite a large scatter in the individual yearly eddy-covariance CUP dates (see insets to Fig. 2), these micrometeorological observations corroborate the atmospheric concentration records.

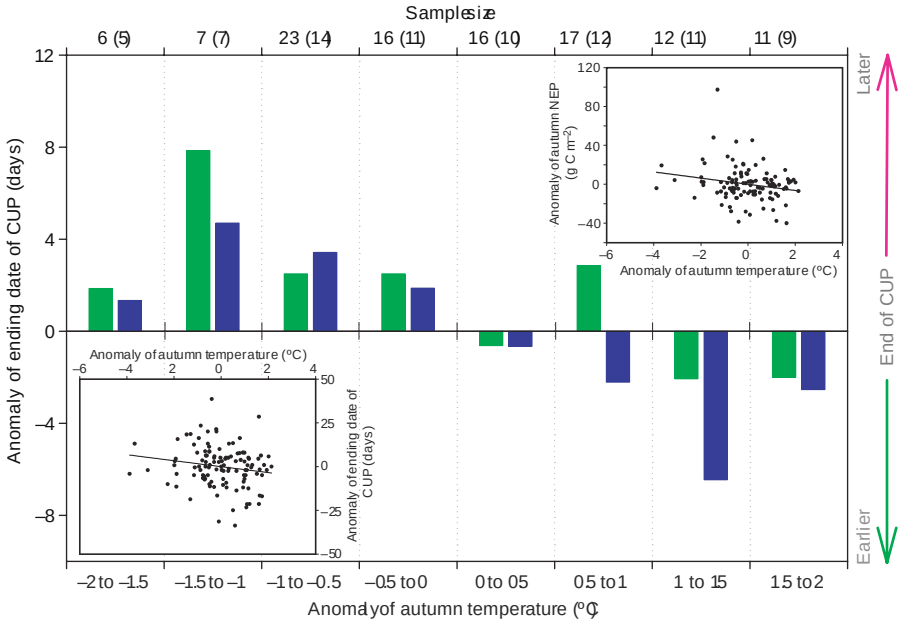

Figure 2 — Eddy-covariance flux data analysis from boreal sites in North America and Eurasia. A total of 108 site-years have been aggregated in this figure. The average (blue) and median (green) anomaly of ending date of net CUP is shown for different autumn temperature anomalies binned into 0.5°C intervals. The top horizontal axis labels correspond to the number of site-years and sites (in parenthesis) in each temperature bin. The bottom left inset shows the relationships between ending date of CUP and temperature anomalies. There is a marginally negative correlation between autumn CUP ending date and temperature anomalies ($y = -1.7x - 0.0087$, $P = 0.07$). If we exclude the four site-years with the most extreme cold anomalies ($\Delta T < -2$°C), the negative correlation between CUP ending date and temperature becomes highly significant ($P = 0.03$) and the slope is steeper ($y = -2.4x + 0.3007$), suggesting that below a certain threshold of cold anomaly there is no further decrease in respiration. The top right inset shows the relationships between autumn NEP and temperature anomalies. A positive NEP value indicates an increased carbon uptake. Autumn was defined as the 60-day interval around the average CUP ending date for each site. Eddy covariance data show increased carbon losses under warmer conditions, with a temperature sensitivity of NEP of -3.2 g C m^{-2} °C^{-1} ($y = -3.17x - 5 \times 10^{-6}$, $P = 0.04$).

The large-scale atmospheric concentration records, taken together with the ecosystem-scale eddy-covariance flux measurements (about 1 km^2) suggest that warmer temperatures in autumn increase ecosystem CO_2 losses by shortening the net CUP. This finding stands in apparent contradiction of the autumn 'greening' and longer-lasting vegetation activity detected at mid-to-high northern latitudes by remote sensing[6,7] and by numerous in situ phenological indicators[13,22]. However, the underlying mechanisms and processes are yet to be explained. NEP results from the balance between gross primary photosynthesis (GPP) and total ecosystem respiration (TER), necessitating separate investigations into the response of each gross flux to temperature changes. We provide some indication of possible controlling mechanisms by using the ORCHIDEE terrestrial biosphere simulation model forced by variable climate fields over the period 1980–2002 (see Methods). The model's ability to capture the timing of the CUP and the length of the growing season successfully was verified by using the following: first, eddy-covariance CO_2 flux measurements[16,23], second, satellite-derived observations of global leaf area index[24], and third, interannual and seasonal variations in atmospheric CO_2 (see Methods and Supplementary Fig. 1). Results

from these studies suggest that it is possible to use this model tool to help in disentangling the response of photosynthesis, respiration and NEP to climate variability.

Simulated September to November NEP shows a trend towards increasing carbon losses in the Northern Hemisphere (north of 25° N) at a rate of 13 Tg C yr^{-1} (P = 0.01) during 1980–2002. In the ORCHIDEE model long-term simulation, the increasing autumn source of carbon to the atmosphere offsets about 90% of the increasing carbon sink in spring. This result is consistent with the atmospheric concentration analysis (Supplementary Table 3). We attribute the trend in net carbon loss during autumn to increases in TER (21 Tg C yr^{-1}) dominating over increasing GPP (8 Tg C yr^{-1} owing to delayed leaf senescence). In autumn, both modelled GPP and TER increase with increasing temperature, but the temperature sensitivity of TER (5.0 g C m^{-2} °C^{-1}) exceeds that of GPP (2.5 g C m^{-2} °C^{-1}). This is due to limitations of radiation and temperature on GPP during the autumn[2,4], and to soil desiccation carried over from the summer dry period[21]. As a result, autumn NEP is simulated to be an increasing source of CO_2 in response to warming, with a mean sensitivity of – 2.5 g C m^{-2} °C^{-1} (or about – 0.2 Pg C °C^{-1} north of 25° N), which is comparable to that derived from eddy-covariance measurements (– 3.2 g C m^{-2} °C^{-1}; Fig. 2).

Our results suggest that net carbon uptake of northern ecosystems is being decreased in response to autumnal warming. The spatial distribution of the response of carbon flux to temperature, as projected by the ORCHIDEE model, is shown in Fig. 3. Warmer autumns coincide with greater than normal GPP (Fig. 3a). However, because of a concurrent stimulation of plant respiration, the geographical area where autumn NPP increases with temperature (slope > 5 g C m^{-2} °C^{-1}) is much less extensive than the area where GPP increases (Fig. 3b). The spatial pattern of the autumn increase in NPP in response to warming is remarkably similar to that of the NOAA/AVHRR vegetation index (NDVI) data[25] (Fig. 3d), suggesting that results from the ORCHIDEE model for NPP are realistic. However, this 'extra' autumn NPP is being accompanied by even more respiration in response to warming, so that the modelled NEP response shows systematic anomalous carbon losses during warmer autumns, in particular over North America and Europe (Fig. 3c).

Observed historical climate data[5] reveal that Eurasia experienced a stronger warming in spring (0.06 °C yr^{-1}, P = 0.001) than in autumn (0.02 °C yr^{-1}, P = 0.15) over the past two decades. In contrast, North America has experienced a larger warming in autumn (0.05 °C yr^{-1}, P = 0.03) than in spring (0.02 °C yr^{-1}, P = 0.36). In addition, a more significant and coherent greening pattern in Eurasia than in North America has been detected in the remote sensing data[7]. This suggests that the processes and the magnitude of seasonal changes in NEP in Eurasia and North America are different, which may control the annual carbon balance of their ecosystems. Further constraints on the spatial and temporal patterns of large-scale ecosystem fluxes will be delivered in the future from atmospheric inversions constrained with longer-term ecosystem flux data.

Applying the future Northern Hemisphere warming of 3.8–6.6 °C predicted by a climate model[26] to the sensitivity of the autumn zero-crossing date of atmospheric CO_2 at Point Barrow (about 5 days °C^{-1}) gives a projected advance of 19–33 days by the end of the twenty-first century. Previous model assessments of the response of land ecosystems to climate change concluded that terrestrial carbon sinks should peak by about the year 2050 and then diminish towards the end of the twenty-first century[9,10]. The asymmetrical impact of autumn versus spring warming on ecosystem carbon exchange contributes significant uncertainty to future projections. If warming in autumn occurs at a faster rate than in spring, the ability of northern ecosystems to sequester carbon may diminish in the future. Acquiring a greater understanding of responses of terrestrial ecosystems to climate trends at the edges of the growing season,

including potential acclimation processes, is clearly a priority, and should come from controlled ecosystem experiments and long-term eddy-covariance data sets.

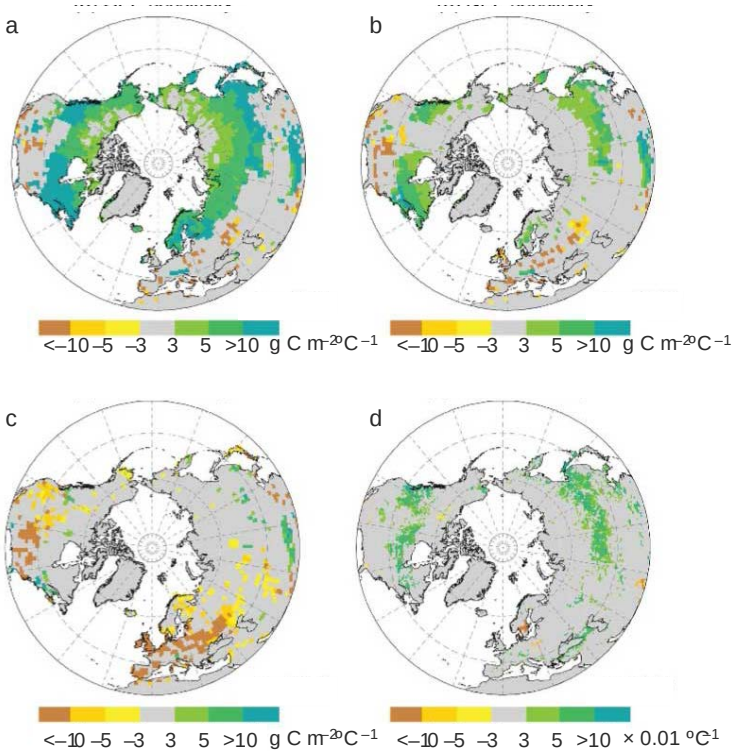

Figure 3 — A model view of the spatial distribution of the effects of autumn (September to November) temperature warming on gross and net carbon fluxes, obtained with the ORCHIDEE model. a, ORCHIDEE model-derived autumn GPP. b, ORCHIDEE model-derived autumn NPP. c, ORCHIDEE model-derived autumn NEP. d, Sum of satellite-derived autumn normalized difference vegetation index (NDVI). The sensitivity is expressed as the linearly regressed slope of autumn carbon flux or of NDVI against autumn temperature for each pixel over the past two decades. A positive slope of NEP indicates that terrestrial carbon uptake is increasing with warmer temperatures, and vice versa. Areas with a low sensitivity or insignificant ($P > 0.05$) relationships between the variables are coloured in grey.

METHODS SUMMARY

We analysed the effects of autumn temperature on the carbon balance of northern ecosystems at different scales, using three different methods.

First, we used smoothed flask CO_2 data from the NOAA/ESRL network[20] to characterize changes in the seasonal CO_2 zero-crossing dates[18,27] for ten stations over the Northern Hemisphere (Fig. 1). We correlated each zero-crossing date with the corresponding observed temperature[5] or precipitation[5] in spring (March to May) and autumn (September to November), and with the ORCHIDEE[16]-modelled soil moisture content. The trends in CO_2 zero-crossing dates and their correlation with climate factors were computed by using linear least-squares regression. The significance of statistical analyses in this study were assessed on the basis of two-tailed significance tests. To isolate further the contribution of fluxes and transport to the year-to-year atmospheric CO_2 signal, we performed factorial simulation experiments in which NEP from the ORCHIDEE[16] vegetation model forced by varying climate fields[5] provided surface boundary conditions for simulated CO_2 in the atmospheric transport model LMDZt[17] driven by interannual winds.

Second, we analysed the net CO_2 flux data measured by the eddy-covariance technique from 24 northern ecosystem sites (Supplementary Table 4). The end of the CUP is defined as the last day in a year when the NEP five-day running means exceed zero. Autumn is defined as the interval of ± 30 days around the average CUP ending date at each site. We grouped the 108 year-site data into distinct 0.5 °C bins of autumn temperature anomaly. For each autumn temperature bin we calculated the median and mean anomaly of the ending date of the CUP.

Third, hints on the processes that control the integrated autumn NEP response to temperature, through the individual sensitivity of photosynthesis and respiration, were provided by integrating the ORCHIDEE vegetation model[16] forced by historic climate data[5] during the period 1980–2002.

References

1. Goulden, M. L. et al. Sensitivity of boreal forest carbon balance to soil thaw. Science 279, 214–217 (1998).
2. Randerson, J. T., Field, C. B., Fung, I. Y. & Tans, P. P. Increases in early season ecosystem uptake explain recent changes in the seasonal cycle of atmospheric CO_2 at high northern latitudes. Geophys. Res. Lett. 26, 2765–2768 (1999).
3. Morgenstern, K. et al. Sensitivity and uncertainty of the carbon balance of a Pacific Northwest Douglas-fir forest during an El Niño La Niña cycle. Agric. For. Meteorol. 123, 201–219 (2004).
4. Bergeron, O. et al. Comparison of carbon dioxide fluxes over three boreal black spruce forests in Canada. Glob. Change Biol. 13, 89–107 (2007).
5. Mitchell, T. D. & Jones, P. D. An improved method of constructing a database of monthly climate observations and associated high-resolution grids. Int. J. Climatol. 25, 693–712 (2005).
6. Myneni, R. B., Keeling, C. D., Tucker, C. J., Asrar, G. & Nemani, R. R. Increased plant growth in the northern high latitudes from 1981 to 1991. Nature 386, 698–702 (1997).
7. Zhou, L. M. et al. Variations in northern vegetation activity inferred from satellite data of vegetation index during 1981 to 1999. J. Geophys. Res. 106, 20069–20083 (2001).
8. Churkina, G., Schimel, D., Braswell, B. H. & Xiao, X. M. Spatial analysis of growing season length control over net ecosystem exchange. Glob. Change Biol. 11, 1777–1787 (2005).
9. Cramer, W. et al. Global response of terrestrial ecosystem structure and function to CO_2 and climate change: results from six dynamic global vegetation models. Glob. Change Biol. 7, 357–373 (2001).
10. Sitch, S. et al. Evaluation of the terrestrial carbon cycle, future plant geography and climate–carbon cycle feedbacks using 5 Dynamic Global Vegetation Models (DGVMs). Glob. Change Biol. (in the press).
11. Black, T. A. et al. Increased carbon sequestration by a boreal deciduous forest in years with a warm spring. Geophys. Res. Lett. 27, 1271–1274 (2000).
12. Tanja, S. et al. Air temperature triggers the recovery of evergreen boreal forest photosynthesis in spring. Glob. Change Biol. 9, 1410–1426 (2003).
13. Menzel, A. et al. European phenological response to climate change matches the warming pattern. Glob. Change Biol. 12, 1969–1976 (2006).
14. Schwartz, M. D., Ahas, R. & Aasa, A. Onset of spring starting earlier across the Northern Hemisphere. Glob. Change Biol. 12, 343–351 (2006).
15. IPCC. Climate Change 2007: The Physical Sciences Basis: Contribution of Working Group I to the Fourth Assessment Report of the Intergovernmental Panel on Climate Change (Cambridge Univ. Press, Cambridge, 2007).
16. Krinner, G. et al. A dynamic global vegetation model for studies of the coupled atmosphere–biosphere system. Glob. Biogeochem. Cycles 19 (2005).
17. Hourdin, F. & Armengaud, A. The use of finite-volume methods for atmospheric advection of trace species. Part I: Test of various formulations in a general circulation model. Mon. Weath. Rev. 127, 822–837 (1999).
18. Keeling, C. D., Chin, J. F. S. & Whorf, T. P. Increased activity of northern vegetation inferred from atmospheric CO_2 measurements. Nature 382, 146–149 (1996).
19. Heimann, M. et al. Evaluation of terrestrial carbon cycle models through simulations of the seasonal cycle of atmospheric CO_2: First results of a model intercomparison study. Glob. Biogeochem. Cycles 12, 1–24 (1998).
20. GLOBALVIEW-CO_2. Cooperative Atmospheric Data Integration Project Carbon Dioxide, ftp.cmdl.noaa.gov/ccg/co2/GLOBALVIEW (2004).
21. Angert, A. et al. Drier summers cancel out the CO_2 uptake enhancement induced by warmer springs. Proc. Natl Acad. Sci. USA 102, 10823–10827 (2005).
22. Linderholm, H. W. Growing season changes in the last century. Agric. For. Meteorol. 137, 1–14 (2006).
23. Ciais, P. et al. Europe-wide reduction in primary productivity caused by the heat and drought in 2003. Nature 437, 529–533 (2005).
24. Piao, S. L., Friedlingstein, P., Ciais, P., Zhou, L. M. & Chen, A. P. Effect of climate and CO_2 changes on the greening of the Northern Hemisphere over the past two decades. Geophys. Res. Lett. 33 (2006).
25. Myneni, R. B. & Song, X. NDVI Version 3 based on Pathfinder, ftp://primavera.bu.edu/pub/datasets/AVHRR_DATASETS/PATHFINDER/VERSION3_DATA/ (2003).
26. Marti, O. et al. The New IPSL Climate System Model: IPSL-CM4 (Institut Pierre Simon Laplace, Paris, 2006).
27. Thoning, K. W., Tans, P. P. & Komhyr, W. D. Atmospheric carbon-dioxide at Mauna Loa Observatory. 2. Analysis of the NOAA GMCC data, 1974–1985. J. Geophys. Res. 94, 8549–8565 (1989).
28. Aubinet, M. et al. Estimates of the annual net carbon and water exchange of forest: the EUROFLUX methodology. Adv. Ecol. Res. 30, 113–175 (2000).

29. Papale, D. et al. Towards a standardized processing of Net Ecosystem Exchange measured with eddy covariance technique: algorithms and uncertainty estimation. Biogeosciences 3, 571–583 (2006).
30. Richardson, C. W. & Wright, D. A. A Model for Generating Daily Weather Variables, Technical Report (US Department of Agriculture, Agricultural Research Service, Washington DC, 1984).
31. van Leer, B. Towards the ultimate conservative difference scheme: IV. A new approach to numerical convection. J. Comput. Phys. 23, 276–299 (1977).
32. Tiedtke, M. A comprehensive mass flux scheme for cumulus parameterization in large-scale models. Mon. Weath. Rev. 117, 1779–1800 (1989).
33. Takahashi, T. et al. in Extended Abstracts of the 2nd International CO in the Oceans Symposium 18–01 (Tsukuba, Japan, 1999).
34. Marland, G., Boden, T. A. & Andres, R. J. Global, Regional, and National CO_2 Emissions. Trends: A Compendium of Data on Global Change. http://cdiac.esd.ornl.gov/trends/emis/tre_glob.htm (2007).
35. Gurney, K. R. et al. Sensitivity of atmospheric CO_2 inversions to seasonal and interannual variations in fossil fuel emissions. J. Geophys. Res. 110 (2005).

Acknowledgements We thank all the people and their respective funding agencies who worked to provide data for this study, and specifically B. Amiro, M. A. Arain, T. A. Black, C. Bourque, L. Flanagan, J. H. McCaughey and S. Wofsy for providing some of the flux data from the Canadian sites, and M.-A. Giasson and C. Coursolle for their help in compiling the data. We also thank A. Friend, P. Rayner and N. Viovy for helpful comments and discussions. This study was supported by European Community-funded projects ENSEMBLES and CARBOEUROPE IP, and by the National Natural Science Foundation of China as well as by Fluxnet-Canada, which was supported by CFCAS, NSERC, BIOCAP, MSC and NRCan. The computer time was provided by CEA. We thank the NOAA-ERSL global air sampling program for collecting and analysing the long-term CO_2 flask data, and K. Masarie at NOAA-ERSL for generating each year the GLOBALVIEW-CO_2 collaborative data product, which formed the basis of our atmospheric data analysis. The ongoing exchange of ideas, data and model results in the international research community on the carbon cycle is facilitated by the Global Carbon Project.

Author Contributions P.C., S.P., P.F. and P.P. designed the research. S.P., P.C. and P.F. performed ORCHIDEE modelling analysis. P.P. and S.P. performed transport analysis. S.P., S.L., M.R., H.M. and P.C. performed eddy-covariance data analysis. S.P., P.C. and J.F. performed satellite data analysis. All authors contributed to the interpretation and writing.

METHODS

Atmospheric CO_2 data. We used flask data from the NOAA/ESRL network to characterize trends in the CO_2 zero-crossing dates (spring downward and autumn CO_2 upward) that correspond roughly to the time of maximum NEP uptake in spring and maximum release in autumn. Following the approach described in ref. 27, we first removed the interannual trend in the atmospheric CO_2 concentration for each site with a polynomial curve of degree 2, four harmonic seasonal function, and time-filtered residuals. We then used the harmonics plus the residuals (detrended CO_2 seasonal cycle) to define the downward and upward CO_2 zero-crossing dates as the day on which the detrended curve crossed the zero line from positive to negative and from negative to positive, respectively. We considered only northern stations for which at least 15 years of data were available during the period 1980–2002 (Supplementary Table 1).

The downward and upward CO_2 zero-crossing dates were correlated with spring (March to May) and autumn (September to November) air temperature[5] over a broad region surrounding each station by 620u of latitude, respectively (Supplementary Table 1). Using a similar method, we also evaluated the correlation with precipitation[5] and modelled change in soil moisture[16].

Eddy-covariance data. The eddy-covariance CO_2 flux observations were performed in accordance with the routine procedures established by regional networks (for example, Fluxnet-Canada and CARBOEUROPE[28]). Half-hourly data were quality-controlled, filtered against low turbulence by using friction velocity as a heuristic criterion and gap-filled by the method developed in ref. 29. Data were aggregated to daily flux integrals and were only used for the analyses if more than 80% of the half-hourly values were either direct measurements or gap-filled with high confidence. The end of the CUP was calculated as the last day in a

year when NEP five-day running means exceeded zero; that is, when the ecosystems became a source of CO_2 to the atmosphere. Autumn was defined as the period during ± 30 days of the average ending date of CUP for each site. Because the flux records are not long enough to assess the long-term impact of autumn temperature trends on the ending date of CUP and net CO_2 exchange for each site, we grouped the 108 year-site data into different 0.5 °C bins of autumn temperature anomaly. For each bin we calculated the median and average anomaly of the ending date of CUP. To ensure the reliability of the statistical analysis of median and average calculation, we used only the data in temperature classes with a sample size greater than 3.

Global vegetation model. The global vegetation model called ORCHIDEE ('ORganizing Carbon and Hydrology In Dynamic Ecosystems')[16] was used to simulate the terrestrial biogeochemical processes. ORCHIDEE describes the turbulent surface fluxes of CO_2, water and energy (transpiration, photosynthesis and respiration), the dynamics of water and carbon pools (soil moisture budget and allocation, growth, mortality, and soil carbon decomposition) and longerterm ecosystem dynamics (fire, sapling establishment and light competition). Fluxes were calculated each hour, and carbon pools were updated each day. Onset and senescence of foliage development depend on a critical leaf age, water and temperature stresses[16].

With the use of 1901 climate data and the 1860 atmospheric CO_2 concentration of 286 p.p.m., a first model spin-up was performed to bring carbon pools to equilibrium. A second spin-up was performed with interannually variable climate data over 1901–1910 to define the initial condition of a run covering 1901– 2002. The monthly climate data sets were supplied by the Climatic Research Unit, University of East Anglia, UK[5]. These data were transformed to half-hourly weather variables by using a weather generator[30].

The modelled NEP over 1980–2002, prescribed in an atmospheric transport model (LMDzt), was found to faithfully reproduce the interannual variations in the spring drawdown date and autumn build-up date at high-latitude (north of 50° N) stations that are predominantly affected by the fluxes of the Northern Hemisphere (Supplementary Table 3 and Supplementary Fig. 1). Furthermore, the modelled upward zero crossing at high-latitude (north of 50° N) stations has advanced by an average of -0.19 ± 0.05 days yr^{-1}, which is comparable to that estimated from atmospheric CO_2 concentration data (-0.22 ± 0.23 days yr^{-1}).

Atmospheric transport model. We used the three-dimensional Eulerian transport model LMDzT derived from the general circulation model of the Laboratoire de Météorologie Dynamique, LMDz[17], to compute the daily CO_2 concentration at each station driven by daily NEP variations from ORCHIDEE during 1980–2002. The model has a horizontal resolution of 3.75° × 2.5° and 19 vertical levels. The simulated winds are relaxed towards the analysed field of ECMWF ('nudging' mode) and therefore vary from year to year according to the observations. Advection, deep convection and turbulent mixing of tracer are calculated by following the schemes proposed in refs 31, 32 and 17, respectively. To separate the effects of transport and terrestrial carbon fluxes on the zero-crossing date signal, we performed two simulations. The first one used interannual daily NEP fluxes calculated during the period 1980–2002 by ORCHIDEE. The second simulation (referred to as 'transport only') used climatological but daily variable NEP. The contribution of interannually varying fluxes to the variability in zero-crossing date is assessed by the difference in simulated atmospheric CO_2 between the first and the second simulations, which is referred to as 'flux only'. In addition, we computed the contribution to CO_2 concentrations from air–sea exchange and fossil fuel emissions and their increase (annual increase per group of countries) by following estimates from refs 33 and 34, respectively. Because of the lack of information on seasonal variations of fossil fuel emissions, we tested the impact of possible changes in fossil seasonality using the method of ref. 35 to construct

seasonally varying fossil fuel emission. We modelled the impact on atmospheric CO_2 in the LMDZt transport model of using a modified fossil fuel source with seasonal amplitude of 40%, 20%, 10%, 5% and 0%. The results showed that the change in zero-crossing date is less than 1.3 days, even when the seasonal amplitude of fossil fuel emissions changed by 40%.

Probability that the observed correlations at several sites happen by chance

We estimated the probability for the correlations between temperature and the zero-crossing dates *interannual variations* at a group of sites, to happen purely by chance. The probability P(*m*,*n*) that the correlation between temperature and zero-crossing date, is negative and fortuitous for *m* of the 10 sites, and that for *n* of these *m* sites, the correlations are significant, can be expressed as follows:

$$P(m,n) = \frac{C_{10}^{m}}{2^{10}} \times C_{m}^{n} \times (2 \times p_s)^{n} \times (1 - 2 \times p_s)^{m-n} \quad \text{(Eq. 1)}$$

$$C_{m}^{n} = \frac{m!}{n!(m-n)!} \quad \text{(Eq. 2)}$$

where, p_s is the probability value (p-value) of a significant correlation using two-tailed significance tests, which generally equals 0.05. The p-value of a statistical hypothesis test is the probability of getting a value of the test statistic as extreme as or more extreme than that observed by chance alone, if the null hypothesis H0, is true. Based on Eq.1, we computed that the probability P(*10,4*) of a fortuitous negative correlation for all 10 sites and significantly negative for exactly 4 of the 10 sites (Table S1) equals $1.1\ 10^{-5}$. Similarly, the probability P(*10,n*) with n > 4 , that is to find a fortuitous significant negative correlation for at least 4 sites, is equal to $1.2\ 10^{-5}$. These results show that the probability of our observed distribution of correlations for ten stations is extremely unlikely to be happening by chance. However, the ten records are not independent (correlated by atmospheric transport for instance), so that the 'group' fortuitous probability maybe higher than the value of P(*m*,*n*). Nevertheless, the group probability value must be less than any p-value of correlation observed for the 10 sites (the

minimum p-value of correlation for 10 sites is 0.002).

Using Eq.1, we also estimated the probability that the *trends* in autumn zero-crossing dates could happen purely by chance. The probability that 8 of the 10 sites show negative trends while 4 of the 8 trends are significant (Table S2) could happen purely by chance is only of $2.0\ 10^{-4}$. The probability that 8 out of 10 sites show negative trends, and that at least 4 out of the 8 trends are significant could happen purely by chance is only $2.2\ 10^{-4}$. This clearly demonstrates that the probability of detecting a significant negative trend at a group of 8 out of 10 stations is very unlikely to be fortuitous.

Table S1. Atmospheric CO_2 measurement sites (data coverage ≥ 15 years) used in this study. DD date: the mean drawdown CO_2 zero-crossing date derived from the interannually detrended atmospheric CO_2 concentration, BU date: the mean upward CO_2 zero-crossing date derived from the interannually detrended atmospheric CO_2 concentration during the study period. At Cape Kumukahi, Sand Island, and Mauna Loa, the upward zero-crossing date of atmospheric CO_2 occurs in the early winter due to the impacts of carbon flux from tropical region.

Station name	abbreviation	Latitude (°N)	Longitude (°E)	DD date (day)	BU date (day)	Period
Alert	ALT	82.45	-62.52	182	323	1988-2002
Barrow	BRW	71.32	-156.60	180	320	1980-2002
Cold Bay	CBA	55.20	-162.72	173	309	1980-1996
Mt. Cimone	CMN	44.18	10.70	155	312	1980-2002
Cape Kumukahi	KUM	19.52	-154.82	193	356	1980-2002
Mould Bay	MBC	76.25	-119.35	184	325	1981-1996
Sand Island	MID	28.22	-117.37	188	347	1985-2002
Mauna Loa	MLO	19.53	-155.58	208	379	1980-2002
Niwot Ridge	NWR	40.05	-105.58	170	334	1980-2000
Schauinsland	SCH	48.00	8.00	145	301	1980-2002

Table S2. Climate variables controlling the zero-crossing date of atmospheric CO_2 in Autumn (upward) and Spring (downward) at ten long-term northern stations of the NOAA/ESRL network. The correlation coefficients values are reported between CO_2 zero-crossing dates at each station, and either temperature, precipitation or soil moisture, the latter being calculated by the ORCHIDEE vegetation model. An asterisk symbol indicates a statistically significant correlation at the 0.05 level. Spring is defined from March through May and Autumn from September through November. Averaged climate variables over a broad land region surrounding each station by ±20 degrees of latitude was used in the correlation analysis. $R_{A\text{-}T}$ is the correlation coefficient of upward zero-crossing date with temperature, $R_{A\text{-}P}$ and $R_{A\text{-}SWC}$ with precipitation and soil moisture respectively. $R_{A\text{-}T/SWC}$ is the coefficient of *partial correlation* between upward zero-crossing dates and temperature, with the controlling effects of soil moisture being removed. $R_{A\text{-}SWC/T}$ is the coefficient of *partial correlation* between upward zero-crossing dates and soil moisture, with the controlling effects of temperature being removed. The upward zero-crossing date for the KUM, MID, and MLO site is also negatively correlated with the mean temperature from October through December, particularly at Cape Kumukahi (R=-0.43, P=0.04) and at Mauna Loa (R=-0.61, P=0.002). The Spring correlation coefficient are denoted by an index S instead of A for Autumn.

Station abbreviation	Latitude (°N)	Longitude (°E)	Autumn					Spring				
			$R_{A\text{-}T}$	$R_{A\text{-}P}$	$R_{A\text{-}SWC}$	$R_{A\text{-}T./SWC}$	$R_{A\text{-}SWC/T}$	$R_{S\text{-}T}$	$R_{S\text{-}P}$	$R_{S\text{-}SWC}$	$R_{S\text{-}T./SWC}$	$R_{S\text{-}SWC/T}$
ALT	82.45	-62.52	-0.33	-0.35	-0.06	-0.34	-0.13	-0.07	-0.61*	-0.42	0.06	-0.42
BRW	71.32	-156.60	-0.61*	-0.27	0.64*	-0.45*	0.51*	-0.83*	-0.22	-0.01	-0.83*	0.04
CBA	55.20	-162.72	-0.45	-0.26	0.41	-0.27	0.21	-0.66*	-0.38	-0.00	-0.66*	-0.07
CMN	44.18	10.70	-0.22	0.18	0.27	-0.04	0.16	0.23	-0.27	-0.14	0.19	-0.05
KUM	19.52	-154.82	-0.41*	-0.14	-0.05	-0.42*	-0.16	-0.45*	-0.07	0.18	-0.44*	0.15
MBC	76.25	-119.35	-0.56*	-0.27	0.27	-0.57*	0.28	-0.67*	-0.30	-0.03	-0.67*	0.10
MID	28.22	-117.37	-0.32	0.03	-0.22	-0.40	-0.33	-0.16	-0.31	0.02	-0.18	-0.00
MLO	19.53	-155.58	-0.52*	-0.06	0.20	-0.50*	0.09	-0.07	0.01	-0.22	-0.09	-0.23
NWR	40.05	-105.58	-0.20	-0.11	-0.06	-0.18	-0.17	0.27	-0.08	-0.27	0.41	-0.12
SCH	48.00	8.00	-0.27	0.27	0.41*	-0.08	0.33	0.07	0.04	0.07	0.11	0.10

Table S3. Trends in the Autumn upward zero-crossing date (Sl_A) and Spring downward zero-crossing date (Sl_S) of atmospheric CO_2 inferred from detrended records at ten long-term northern stations (data coverage > 15 years) of the NOAA/ESRL network. A negative trend indicates an earlier zero-crossing date. The trend in the length of the Carbon Uptake Period, Sl_{CUP}, is defined by $Sl_{CUP} = Sl_A - Sl_S$. Sl_{A-W} is the modeled trend autumn zero-crossing date caused by variable atmospheric transport only. Its value is determined by prescribing climatological NEP fluxes from the ORCHIDEE vegetation model into the LMDZt global atmospheric transport model with interannual winds over the period 1980-2002 (see methods). R_{A-W} is the correlation coefficient between the observed and the 'transport-only' modeled Autumn zero-crossing date. A significant high value for R_{A-W} hence indicates that atmospheric transport explains a great part of observed the zero crossing date signals, which is not the case. R_{A-F} is the correlation coefficient between the observed and the modeled Autumn CO_2 zero-crossing date caused by variable NEP fluxes from the ORCHIDEE vegetation model only, referred to as the 'flux -only' zero-crossing dates (see methods). The Spring correlation coefficient are denoted by an index S instead of A for Autumn.

Station abbreviation	Latitude (°N)	Longitude (°E)	Autumn				Spring				Sl_{CUP} (day yr^{-1})	Sl_{CUP-W} (day yr^{-1})
			Sl_A (day yr^{-1})	Sl_{A-W} (day yr^{-1})	R_{A-W}	R_{A-F}	Sl_S (day yr^{-1})	Sl_{S-W} (day yr^{-1})	R_{S-W}	R_{S-F}		
ALT	82.45	-62.52	-0.15	0.06	0.54*	0.58*	-0.09	0.06	0.06	0.82*	-0.06	0.00
BRW	71.32	-156.60	-0.40*	-0.12	0.39	0.69*	-0.26*	-0.07	0.41*	0.73*	-0.14	-0.05
CBA	55.20	-162.72	0.07	0.02	0.36	0.56*	-0.11	-0.09	0.60*	0.69*	0.18	0.11
CMN	44.18	10.70	-0.05	0.08	0.15	-0.13	0.27	0.57	-0.06	0.03	-0.32	-0.49
KUM	19.52	-154.82	-0.91*	-0.11	0.41*	-0.21	-0.31*	0.05	0.36	0.54*	-0.60*	-0.16
MBC	76.25	-119.35	-0.42	0.08	0.41	0.53*	-0.22	-0.02	0.18	0.70*	-0.20	0.10
MID	28.22	-117.37	-1.08*	0.23	-0.11	0.16	-0.27	0.07	0.28	0.30	-0.81	0.16
MLO	19.53	-155.58	-0.76*	0.12	-0.22	0.50*	-0.08	0.08	0.34	0.38	-0.68*	0.04
NWR	40.05	-105.58	0.67	0.04	0.16	0.26	0.72*	0.44	0.07	0.02	-0.05	-0.40
SCH	48.00	8.00	-0.54	0.07	0.00	0.06	0.43	0.01	0.07	-0.04	-0.97*	0.06

Table S4. Eddy-covariance CO_2 measurement sites used in this study.

Site Code	Name	Country	Latitude	Longitude	Vegetation type	Period
Ca-DF49	Campbell River	Canada	49.87	-125.33	ENF	1997-2005
Ca-HDF00	Campbell River	Canada	49.87	-125.29	ENF	2000-2005
Ca-HDF89	Campbell River	Canada	49.53	-124.90	ENF	2001-2005
Ca-Grass	Lethbridge	Canada	49.71	-112.94	Grassland	1998-2005
Ca-EP	Eastern Peatland (Mer Bleue)	Canada	45.41	-75.48	Raised bog	1998-2005
Ca-BF	New Brunswick Balsam Fir	Canada	46.47	-67.10	ENF	2003-2005
Ca-NOBS	Northern Old Black Spruce	Canada	55.88	-98.48	ENF	1995-2003
Ca-OA	BERMS Old Aspen	Canada	53.63	-106.20	BDF	1997-2005
Ca-OMW	Ontario Mixedwood	Canada	48.22	-82.15	Mixed forest	2003-2005
Ca-SOBS	BERMS Southern Old Black Spruce	Canada	53.99	-105.12	ENF	1999-2005
Ca-SOJP	BERMS Southern Old jack Pine	Canada	53.92	-104.69	ENF	1999-2005
Ca-HBS00	Quebec Cutover	Canada	49.27	-74.04	ENF	2001-2005
Ca-EOBS	Eastern Old Black Spruce	Canada	49.69	-74.34	ENF	2003-2005
Ca-F77	BERMS fire 1977	Canada	54.49	-105.82	ENF	2003-2005
Ca-F89	BERMS fire 1989	Canada	54.25	-105.88	Woody savannas	2003-2005
Ca-F98	BERMS fire 1998	Canada	54.09	-106.01	Open shrubland	2003-2005
Ca-HJP02	BERMS Harvested Jack Pine	Canada	53.88	-104.65	ENF	2004-2005
Ca-WPP	White Pine Plantation (Turkey Point)	Canada	42.71	-80.36	ENF	2003-2005
Ca-WP	Western Peatland	Canada	54.95	-112.47	Treed Fen	2003-2005
FI-Hyy	Hyytiälä	Finland	61.85	24.30	ENF	1996-2005
FI-Kaa	Kaamanen	Finland	69.14	27.30	Wetland	2000-2005
FI-Sod	Sodankylä	Finland	67.36	26.64	ENF	2001-2005
SE-Nor	Norunda	Sweden	60.09	17.48	ENF	1996-2005
SE-Fla	Flakaliden	Sweden	64.12	19.45	ENF	1996-2002
US-Ho1	Howland	USA	45.20	-68.74	Mixed forest	1996-2004

ENF: Evergreen needleleaf forest; BDF: Broadleaf deciduous forest.

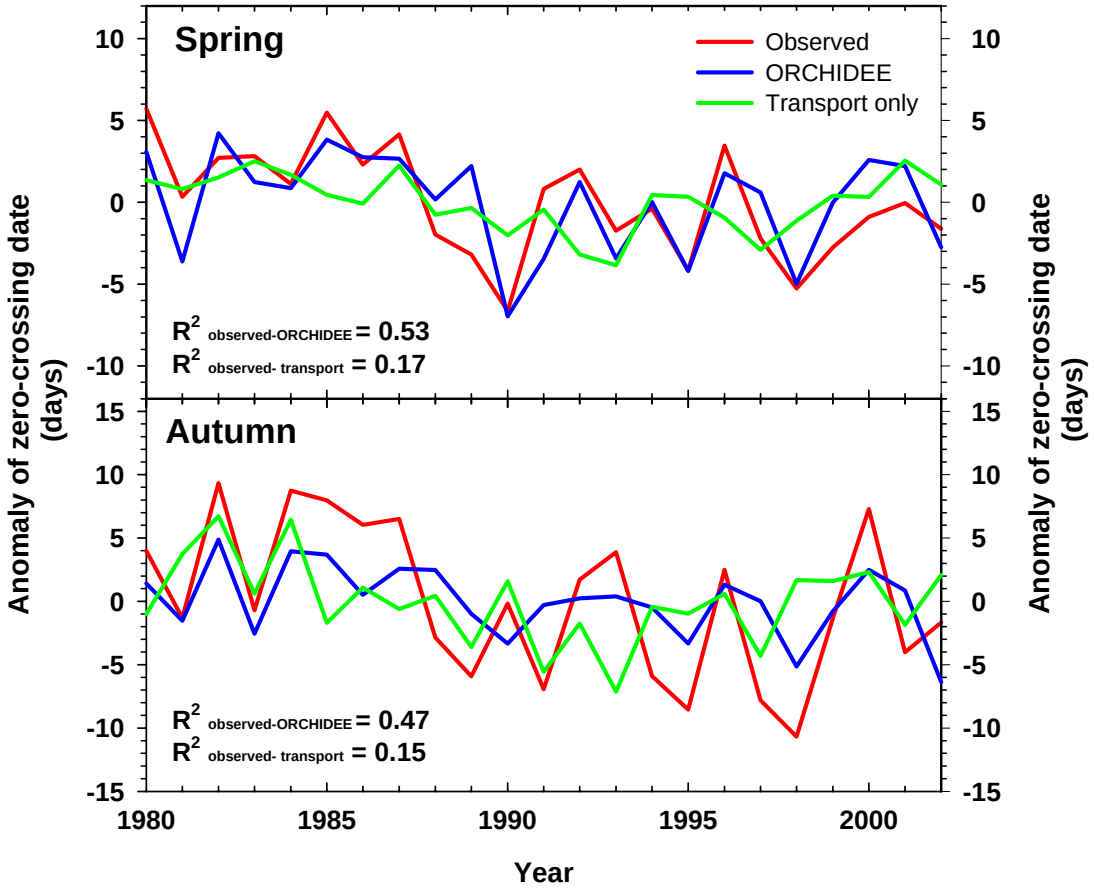

Figure S1. Interannual variations zero-crossing dates at Point Barrow (longitude -156.6 ^{o}E; latitude 71.32 ^{o}N) in northern Alaska. Red = observed zero-crossing dates from the NOAA/ESRL observations. Blue = modeled 'flux-only' zero-crossing dates obtained by taking the difference between 1) a simulation where variable NEP fluxes from the ORCHIDEE vegetation model over 1980-2002 is prescribed to the LMDZt transport model with variable wind fields and 2) another simulation where climatological NEP from ORCHIDEE is prescribed to LMDZt. The LMDZ model output has been sampled at the grid-point of the Point-Barrow station. Green = modeled 'transport only' zero-crossing dates obtained when climatological NEP from ORCHIDEE is prescribed to the LMDZt transport model with variable wind fields. About 50% of the observed zero-crossing date variance can be explained by NEP variability, against only about 15% by atmospheric transport changes.